The energy and helicity of knotted magnetic flux tubes

By A.Y.K. Chui and H.K. Moffatt

Department of Applied Mathematics and Theoretical Physics, University of Cambridge, Silver Street, Cambridge CB3 9EW, U.K.

Magnetic relaxation of a magnetic field embedded in a perfectly conducting incompressible fluid to minimum energy magnetostatic equilibrium states is considered. It is supposed that the magnetic field is confined to a single flux tube which may be knotted. A local non-orthogonal coordinate system, zero-framed with respect to the knot, is introduced, and the field is decomposed into toroidal and poloidal ingredients with respect to this system. The helicity of the field is then determined; this vanishes for a field that is either purely toroidal or purely poloidal. The magnetic energy functional is calculated under the simplifying assumptions that the tube is axially uniform and of circular cross-section. The case of a tube with helical axis is first considered, and new results concerning kink mode instability and associated bifurcations are obtained. The case of flux tubes in the form of torus knots is then considered and the 'ground-state' energy function $\overline{m}(h)$ (where h is an internal twist parameter) is obtained; as expected, $\overline{m}(h)$, which is a topological invariant of the knot, increases with increasing knot complexity. The function $\overline{m}(h)$ provides an upper bound on the corresponding function $m(h)$ that applies when the above constraints on tube structure are removed. The technique is applicable to any knot admitting a parametric representation, on condition that points of vanishing curvature are excluded.

1. Introduction

Stable magnetostatic equilibria of perfectly conducting fluids are characterised by the fact that the energy of the system (magnetic plus internal) is minimal with respect to 'frozen-field' distortions, i.e. virtual displacements which convect the magnetic field in such a way that its flux through every material surface element is conserved (Bernstein *et al* 1958). This principle provides a basis for the study of stability of toroidal equilibria as realised in toroidal plasma devices such as the TOKAMAK, and of magnetostatic structures in astrophysics (e.g. coronal loops above the solar photosphere).

If a localised magnetic field structure imbedded in a perfectly conducting fluid is not in magnetostatic equilibrium (i.e. if the Lorentz force $\mathbf{j} \times \mathbf{B}$ is not irrotational so that it cannot be balanced by pressure gradient alone) then it will tend to 'relax' towards a minimum energy state, the field topology being conserved (Arnol'd 1974, Moffatt 1985). This process requires that some mechanism

Phil. Trans. R. Soc. Lond. A (1995) ???, 1–22

of energy dissipation (other than Joule dissipation) be present; the natural mechanism is that of viscosity which operates when the fluid is in motion, and ceases to operate when the minimum energy magnetostatic state is attained.

A particularly interesting situation arises if the field $\mathbf{B}$ is confined to a single closed flux tube which may be knotted in the form of a knot $\mathcal{K}$ (for examples, see Figures 4, 8, below). We shall suppose that the field lines lie on a family of surfaces $\chi = \text{cst.}$ $(0 \leqslant \chi \leqslant 1)$ nested around the axis C of the tube (which is itself a closed field line in the form of the knot $\mathcal{K}$). Let V be the volume of the tube and let Φ be the flux of $\mathbf{B}$ across any cross-section. It has been shown (Moffatt 1990a) that if such a tube is constructed in a standard way with uniform axial field in the tube and net angle of twist $2\pi h$ of the field around C (a construction that will be made precise in §4 below), then the helicity of the field is $\mathcal{H} = h\Phi^2$ and the minimum energy that can be attained under frozen-field volume-preserving distortions (isotopies) (as realisable in an incompressible fluid) has the form

$$\mathcal{M}_{\min} = m(h)\Phi^2 V^{-\frac{1}{3}}, \tag{1.1}$$

where $m(h)$ is a function determined (in principle) solely by the topology of $\mathcal{K}$. Nontrivial topology of $\mathcal{K}$ and/or nonzero twist h guarantee that $m(h) > 0$ (Freedman 1988). An explicit lower bound on $m(h)$ in terms of crossing number is given by Freedman & He (1991). Eqn.(1.1) is in effect a dimensional necessity, the quantities Φ, V and h being invariant during the distortion process. The dimensionless function $m(h)$ may be described as the 'ground-state' energy function for $\mathcal{K}$; more generally, there may exist a set of functions

$$\{m_0(h)\,,\ m_1(h)\,,\ m_2(h)\,,\ \ldots\} \tag{1.2}$$

corresponding to different local minima, which may be described as the 'energy spectrum' of $\mathcal{K}$.

Determination of the function $m(h)$ for given $\mathcal{K}$ is a fundamental objective which is beyond the power of current super-computers. We address the problem in the present paper by placing additional mild constraints on the field structure, by means of which considerable analytical progress may be made. Specifically, we shall suppose (in §5 *et seq*) that the magnetic surfaces $\chi = \text{cst.}$ are of circular cross-section and invariant along the tube axis. These assumptions permit reduction of the expression for $\mathcal{M}$ to a form for which computational minimisation is straightforward. We illustrate the procedure in §8 for the family of torus knots. Due to the additional constraints introduced, the function $\overline{m}(h)$ obtained by this technique can be regarded only as an upper bound for $m(h)$; but we believe that this provides a reasonable approximation to $m(h)$ provided $|h|$ is not too large, and that the behaviour revealed by $\overline{m}(h)$ is then qualitatively 'correct'.

The key technique in our approach is the use of a non-orthogonal coordinate system (s, χ, ϕ) specially adapted to the problem; s is arclength on C, χ is the flux function introduced above, and ϕ is a polar angle in the cross-section of the tube with the special 'zero-framing' property that the ribbon $\phi = 0$ is untwisted, i.e. the curve $C(\chi = 0)$ and the curve $\{\phi = 0, \chi = 1\}$ have zero linking number. This essential property allows for an unambiguous decomposition of $\mathbf{B}$ into toroidal (or axial) and poloidal (or meridional) ingredients, and the helicity $\mathcal{H}$ of the field is then expressible as a function of toroidal and poloidal fluxes (Eqn. (3.14) below). A result of this type was obtained by Kruskal & Kulsrud (1958) and by

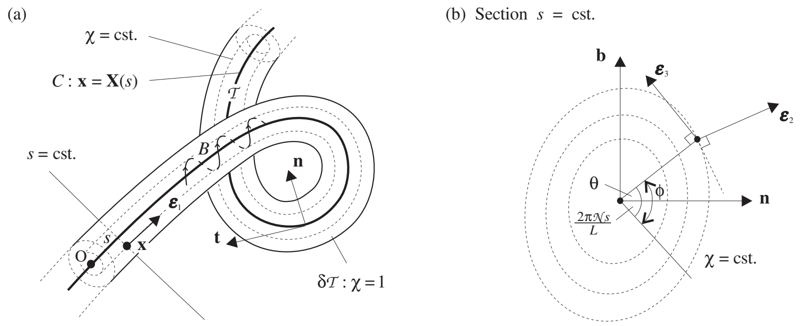

Figure 1. (a) Portion of a flux tube $\mathcal{T}$ with magnetic axis C and magnetic surfaces $\chi = \text{cst.}$ (b) Section $s = \text{cst.}$ of flux tube.

Berger & Field (1984); but the present paper makes it clear that the result is valid for knotted tubes only if the toroidal/poloidal decomposition is defined via the zero-framed coordinate system as indicated above.

This paper provides a natural development of an earlier preliminary study (Chui & Moffatt 1992) in which the ground-state energy function $m(h)$ of an *unknotted* closed flux tube was determined, on the assumption that the minimising configuration is axi-symmetric. Kink mode instabilities may invalidate this assumption. The techniques developed below are well-adapted to the identification of new helical equilibrium (or near-equilibrium) states consequent upon such instabilities. This problem is briefly treated in §6 for two cylindrical configurations ('free' and 'line-tied'), and analytical results are obtained which are in broad agreement with earlier studies of Anzer (1968) and Hood & Priest (1979). This theme will be more fully developed in a separate paper.

2. Flux coordinates and zero-framing

Our first objective is to introduce an appropriate coordinate system to describe a magnetic field $\mathbf{B}$ which is confined to a closed, possibly knotted, flux tube $\mathcal{T}$ of small cross-section. Obviously we must suppose that this tube is nowhere self-intersecting. We shall suppose further that the lines of force of $\mathbf{B}$ (or '$\mathbf{B}$-lines') lie on a family of nested surfaces $\chi(\mathbf{x}) = \text{cst.}$ within $\mathcal{T}$, where χ takes values in the range $0 \leqslant \chi \leqslant 1$. These surfaces will be denoted S_χ. The innermost (degenerate) surface $\chi = 0$ is a closed curve C, the 'magnetic axis' (Figure 1a). The outermost surface $\chi = 1$ is $\partial\mathcal{T}$, the boundary of $\mathcal{T}$. A possible choice for χ is

$$\chi = V/V_{\mathcal{T}}\,, \tag{2.1}$$

where V is the volume inside the surface labelled χ and $V_{\mathcal{T}}$ is the volume of the whole tube $\mathcal{T}$; but clearly this is not the only possibility.

Let s represent arclength on C measured from some arbitrary point of C, and let $\mathbf{X}(s)$ be the parametric representation of points of C. Since C is a closed curve,

$$\mathbf{X}(s+L) = \mathbf{X}(s)\,, \tag{2.2}$$

where L is the length of C. Let $c(s)$, $\tau(s)$ be the curvature and torsion of C. We

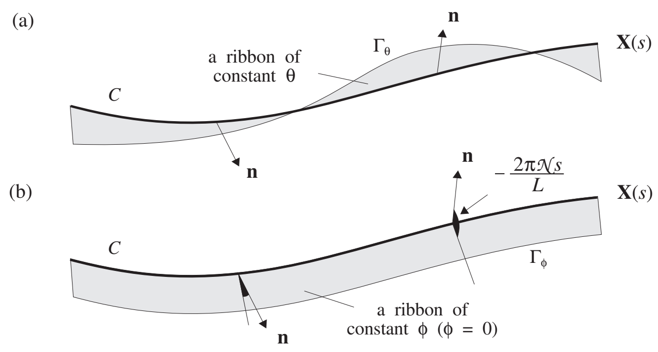

Figure 2. (a) Ribbon $\theta = \text{cst.}$ with boundaries C and Γ_θ which have linking number $\mathcal{N}$. (b) Ribbon $\phi = \text{cst.}$ with boundaries C and Γ_ϕ which have zero linking number.

shall suppose, unless otherwise stated, that

$$c(s) > 0 \quad \text{(for all } s\text{)}, \tag{2.3}$$

i.e. that C has no points of inflexion. Let $\mathbf{t} = d\mathbf{X}/ds$ be the unit tangent vector, $\mathbf{n}$ the unit principal normal, and $\mathbf{b} = \mathbf{t} \wedge \mathbf{n}$ the unit binormal, satisfying the Frenet equations

$$\frac{d\mathbf{t}}{ds} = c\mathbf{n}\,, \quad \frac{d\mathbf{n}}{ds} = -c\mathbf{t} + \tau\mathbf{b}\,, \quad \frac{d\mathbf{b}}{ds} = -\tau\mathbf{n}\,. \tag{2.4}$$

Clearly an arbitrary point $\mathbf{x}$ in $\mathcal{T}$ may be expressed in the form

$$\mathbf{x} = \mathbf{X}(s) + r\cos\theta\,\mathbf{n} + r\sin\theta\,\mathbf{b}\,, \tag{2.5}$$

where (r, θ) are plane polar coordinates in the plane through $\mathbf{X}(s)$ defined by the vectors $(\mathbf{n}, \mathbf{b})$ with θ measured from the direction of $\mathbf{n}$ (Figure 1b).

Consider a 'ribbon surface' $\theta = \text{cst.}$, $0 \leqslant \chi \leqslant 1$ (Figure 2a). The boundaries of this ribbon are the curve C and its curve of intersection Γ_θ with $\partial\mathcal{T}$. If the tube is knotted, then in general C and Γ_θ are linked. Let $\mathcal{N}$ be the Gauss linking number of (C, Γ_θ) which may be positive or negative (or exceptionally zero); in constructing $\mathcal{N}$, we adopt the same orientation of C and Γ_θ going the long way round the tube $\mathcal{T}$.

We now define a new angle variable

$$\phi = \theta + 2\pi\mathcal{N}s/L\,. \tag{2.6}$$

This has the property that the ribbon $\phi = \text{cst.}$ (i.e. $\theta = \text{cst.} - 2\pi\mathcal{N}s/L$) is 'untwisted' in the sense that its boundaries C at $\chi = 0$ and Γ_ϕ at $\chi = 1$ have zero linking number (Figure 2b). Choice of ϕ (rather than θ) as the appropriate angle variable is what topologists describe as 'zero-framing'.

Through each point (s, r, ϕ), there is a unique magnetic surface, i.e.

$$\chi = \chi(s, r, \phi)\,. \tag{2.7}$$

We shall suppose that we may invert uniquely for r in the form

$$r = R(s, \chi, \phi)\,. \tag{2.8}$$

(This requires merely that the surfaces $\chi = \text{cst.}$ are not folded upon themselves within $\mathcal{T}$.) It is convenient to use χ as a coordinate in place of r, because by definition $\mathbf{B}\cdot\nabla\chi = 0$, so that $\mathbf{B}$ has no component in the direction of $\nabla\chi$. $R(s,\chi,\phi)$ may be described as the *shape-function* of the flux tube.

We now adopt (s,χ,ϕ) as our system of coordinates, so that (2.5) becomes

$$\begin{aligned}\mathbf{x} = \mathbf{X}(s) &+ R(s,\chi,\phi)\cos(\phi - 2\pi\mathcal{N}s/L)\mathbf{n}(s)\\ &+ R(s,\chi,\phi)\sin(\phi - 2\pi\mathcal{N}s/L)\mathbf{b}(s)\,.\end{aligned} \tag{2.9}$$

Let us consider the fundamental properties of this system (for relevant background concerning non-orthogonal coordinate systems, see Bradbury 1984). Note first that

$$d\mathbf{x} = \mathbf{e}_1 ds + \mathbf{e}_2 d\chi + \mathbf{e}_3 d\phi\,, \tag{2.10}$$

where the basis vectors $\mathbf{e}_1, \mathbf{e}_2, \mathbf{e}_3$ are given by

$$\begin{cases}\mathbf{e}_1 &= (1 - Rc\cos\theta)\mathbf{t} + (R_s\cos\theta - R\tau^*\sin\theta)\mathbf{n} + (R_s\sin\theta + R\tau^*\cos\theta)\mathbf{b}\,,\\ \mathbf{e}_2 &= R_\chi(\cos\theta\,\mathbf{n} + \sin\theta\,\mathbf{b})\,,\\ \mathbf{e}_3 &= (-R\sin\theta + R_\phi\cos\theta)\mathbf{n} + (R\cos\theta + R_\phi\sin\theta)\mathbf{b}\,,\end{cases} \tag{2.11}$$

with

$$\theta = \phi - 2\pi\mathcal{N}s/L\,, \quad \tau^*(s) = \tau(s) - 2\pi\mathcal{N}/L\,. \tag{2.12}$$

Note that $\mathbf{e}_1$ is dimensionless, while $\mathbf{e}_2$ and $\mathbf{e}_3$ have the dimensions of length. The metric tensor is

$$(g_{ij}) = (\mathbf{e}_i\cdot\mathbf{e}_j) = \begin{pmatrix}(1 - Rc\cos\theta)^2 + R^2\tau^{*^2} + R_s^2 & R_\chi R_s & R^2\tau^* + R_sR_\phi\\ R_\chi R_s & R_\chi^2 & R_\chi R_\phi\\ R^2\tau^* + R_sR_\phi & R_\chi R_\phi & R^2 + R_\phi^2\end{pmatrix} \tag{2.13}$$

so that the coordinate system (s,χ,ϕ) is clearly in general non-orthogonal. The determinant of (g_{ij}) is

$$g = R^2\,R_\chi^2\,(1 - Rc\cos\theta)^2, \tag{2.14}$$

and the Jacobian of the transformation to coordinates (s,χ,ϕ) is

$$J = (\mathbf{e}_1\wedge\mathbf{e}_2)\cdot\mathbf{e}_3 = \sqrt{g} = RR_\chi(1 - Rc\cos\theta)\,. \tag{2.15}$$

Thus $J > 0$ and the transformation is well defined provided

$$rc(s) < 1 \quad \text{all } s, \text{ all } \mathbf{x}\in\mathcal{T}, \tag{2.16}$$

i.e. provided $\mathcal{T}$ has sufficiently small cross-section. We shall assume (2.16) to be satisfied.

Since $\mathbf{B}\cdot\nabla\chi = 0$, the field $\mathbf{B}$ has only two components relative to the system (s,χ,ϕ):

$$\mathbf{B} = B^1\mathbf{e}_1 + B^3\mathbf{e}_3\,. \tag{2.17}$$

The condition $\nabla\cdot\mathbf{B} = 0$ implies that

$$\frac{\partial}{\partial s}(\sqrt{g}B^1) + \frac{\partial}{\partial\phi}(\sqrt{g}B^3) = 0\,. \tag{2.18}$$

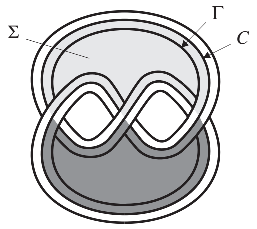

Figure 3. Siefert surface Σ for the trefoil knot, intersecting the tube surface in the curve Γ; Σ^* is that part of Σ outside $\mathcal{T}$.

Hence there exists a flux function $\psi(s,\chi,\phi)$ such that

$$B^1 = -\frac{1}{\sqrt{g}}\,\frac{\partial\psi}{\partial\phi}\,, \quad B^3 = \frac{1}{\sqrt{g}}\,\frac{\partial\psi}{\partial s}\,. \tag{2.19}$$

By analogy with the terminology for an unknotted flux tube in the form of a torus, we define

$$\mathbf{B}_T = B^1\mathbf{e}_1\,, \quad \mathbf{B}_P = B^3\mathbf{e}_3\,, \tag{2.20}$$

as, respectively, the toroidal and poloidal ingredients of $\mathbf{B}$. Let $T(\chi)$ be the toroidal flux across any section $s =$ cst. inside S_χ, and let $P(\chi)$ be the poloidal flux across any ribbon $\phi =$ cst. bounded by the magnetic axis C and S_χ. Then (cf. Bateman 1978, pp. 127–128)

$$\psi(s,\chi,\phi) = \tilde{\psi}(s,\chi,\phi) - \frac{\phi}{2\pi}\,\frac{dT}{d\chi} + \frac{s}{L}\,\frac{dP}{d\chi}\,, \tag{2.21}$$

where $\tilde{\psi}(s,\chi,\phi)$ is a single-valued function, periodic in s (with period L) and in ϕ (with period 2π). Hence from (2.17) and (2.19),

$$\mathbf{B} = \frac{1}{\sqrt{g}}\left(\frac{1}{2\pi}T'(\chi),\, 0,\, \frac{1}{L}P'(\chi)\right) + \frac{1}{\sqrt{g}}\left(-\frac{\partial\tilde{\psi}}{\partial\phi}\,,\, 0\,,\, \frac{\partial\tilde{\psi}}{\partial s}\right)\,. \tag{2.22}$$

Here, the first term is the 'mean' field with prescribed fluxes, and the second term is the 'fluctuation' field with zero net fluxes.

3. The helicity of a flux tube

The helicity of the field $\mathbf{B}$ is

$$\mathcal{H} = \int_{\mathcal{T}} \mathbf{A}\cdot\mathbf{B}\,dV\,, \tag{3.1}$$

where $\mathbf{A}$ is a vector potential of $\mathbf{B}$, i.e. $\mathbf{B} =$ curl $\mathbf{A}$. We must impose upon $\mathbf{A}$ a condition that guarantees that the magnetic flux threading the space $\mathcal{T}^*$ outside $\mathcal{T}$ is zero. Let Σ be a Siefert surface (two-sided and non-self-intersecting) of C (Figure 3) (see, for example, Scharlemann 1992). Let Γ be the curve of intersection of Σ and $\partial\mathcal{T}$. The linking number of any closed curve C^* with C may be computed as the algebraic sum of the number of crossings of Σ by C^* (taking account of the sense of crossing). If C^* lies wholly on Σ, then the linking number of C and C^* is zero. Hence in particular the linking number of Γ and C

is zero, and so Γ may be deformed continuously on $\partial\mathcal{T}$ to coincide with Γ_ϕ, the intersection of $\phi = 0$ and $\partial\mathcal{T}$. Now let Σ^* be the part of Σ bounded by Γ_ϕ and lying entirely in $\mathcal{T}^*$. Plainly, the flux of $\mathbf{B}$ across Σ^* is zero, i.e.

$$\int_{\Sigma^*} \mathbf{B}\cdot\mathbf{n}\, dS = \oint_{\Gamma_\phi} \mathbf{A}\cdot d\mathbf{x} = \int_0^L A_1(s,1,0)ds = 0\,. \tag{3.2}$$

This is the condition that $\mathbf{A}$ must satisfy; subject to this constraint and to prescribed toroidal flux Φ, the helicity integral (3.1) is gauge-invariant. (Note that (3.2) is satisfied for knotted tubes precisely because the linking number of Γ_ϕ and C is zero; it is *not* satisfied if coordinates (r,χ,θ) are used instead of (r,χ,ϕ).)

The form (2.22) of $\mathbf{B}$ allows us to seek a vector potential of the form $\mathbf{A} = (A_1, 0, A_3)$ where, from $\mathbf{B} = \text{curl}\ \mathbf{A}$,

$$\sqrt{g}B^1 = \frac{\partial A_3}{\partial\chi}\,, \quad 0 = \frac{\partial A_1}{\partial\phi} - \frac{\partial A_3}{\partial s}\,, \quad \sqrt{g}B^3 = -\frac{\partial A_1}{\partial\chi}\,. \tag{3.3}$$

Let

$$\eta(s,\chi,\phi) = \int_0^\chi \tilde{\psi}(s,\chi,\phi)\, d\chi\,; \tag{3.4}$$

like $\tilde{\psi}$, this function is single-valued and periodic in s and ϕ. From (3.3) and (2.22), we then find

$$\begin{cases} A_1 &= -\eta_s(s,\chi,\phi) - L^{-1}P(\chi) + C_1(s,\phi)\,, \\ A_3 &= -\eta_\phi(s,\chi,\phi) + (2\pi)^{-1}T(\chi) + C_3(s,\phi)\,, \end{cases} \tag{3.5}$$

where C_1 and C_3 are 'constants of integration'. Choosing $C_3 = 0$ ensures that $\mathbf{A}$ is continuous at $\chi = 0$; and choosing $C_1 = P(1)/L$ ensures that the condition (3.2) is satisfied. This gives then

$$A_1 = -\eta_s + \tilde{P}/L\,, \quad A_3 = -\eta_\phi + T/2\pi\,, \tag{3.6}$$

where $\tilde{P}(\chi) = P(1) - P(\chi)$ is the 'complementary' poloidal flux across a ribbon $\phi = \text{cst.}$ *outside* S_χ.

Now let

$$\mathcal{H}(\chi^*) = \int_{\chi<\chi^*} \mathbf{A}\cdot\mathbf{B}\, dV = \iiint_{\chi<\chi^*} (A_1B^1 + A_3B^3)\sqrt{g}\, ds\, d\chi\, d\phi \tag{3.7}$$

be the helicity inside S_{χ^*}. Equivalently,

$$\frac{d\mathcal{H}}{d\chi} = \iint (A_1B^1 + A_3B^3)\sqrt{g}\, ds\, d\phi\,. \tag{3.8}$$

Substituting from (3.6) and (2.22), we have

$$\frac{d\mathcal{H}}{d\chi} = \iint \left(-\eta_s + \frac{\tilde{P}}{L}\right)\left(-\eta_{\phi\chi} + \frac{T'}{2\pi}\right) + \left(-\eta_\phi + \frac{T}{2\pi}\right)\left(\eta_{s\chi} - \frac{\tilde{P}'}{L}\right) ds\, d\phi\,. \tag{3.9}$$

Here terms linear in the derivatives of η integrate to zero because η is periodic in s and in ϕ. Hence

$$\frac{d\mathcal{H}}{d\chi} = \iint (\eta_s\eta_{\phi\chi} - \eta_\phi\eta_{s\chi})\, ds\, d\phi + \left(T'\tilde{P} - T\tilde{P}'\right)\,. \tag{3.10}$$

Now, by integrating by parts,

$$\iint \eta_\phi \eta_{s\chi}\, ds\, d\phi = -\iint \eta_{\phi s}\eta_\chi\, ds\, d\phi = \iint \eta_s \eta_{\phi\chi}\, ds\, d\phi\,, \tag{3.11}$$

where we again use the periodicity of η in s and ϕ. Hence (3.10) becomes simply

$$\frac{d\mathcal{H}}{d\chi} = T'\tilde{P} - T\tilde{P}', \tag{3.12}$$

or equivalently

$$\mathcal{H}(\chi^*) = \int_0^{\chi^*} \left(T'\tilde{P} - T\tilde{P}'\right) d\chi\,. \tag{3.13}$$

Thus the helicity inside each magnetic surface S_χ is determined solely by the toroidal and (complementary) poloidal flux functions $T(\chi)$ and $\tilde{P}(\chi)$.

A result equivalent to (3.12) was obtained by Kruskal & Kulsrud (1958), and by Berger & Field (1984) by an argument based on linkage of field lines for the case of an unknotted tube. From the discussion of this section, however, it emerges that the result is true also of a knotted flux tube, provided the poloidal field is properly defined through use of a zero-framed coordinate system.

The total helicity is

$$\mathcal{H}_{\text{tot}} = \mathcal{H}(1) = \int_0^1 (T'\tilde{P} - T\tilde{P}')\, d\chi = 2\int_0^1 T(\chi)P'(\chi)\, d\chi\,, \tag{3.14}$$

using integration by parts. For a field with uniform twist h, $P(\chi) = hT(\chi)$, and (3.14) becomes

$$\mathcal{H}_{\text{tot}} = 2h\int_0^1 T(\chi)T'(\chi)\, d\chi = h\Phi^2\,, \tag{3.15}$$

where $\Phi = T(1)$ is the total toroidal flux. The result (3.15) is already known for unknotted twisted flux tubes (Moffatt 1990a); here we have shown it to be equally true for knotted flux tubes, provided again that the poloidal flux is defined as the flux through a ribbon (ϕ = cst.) which is not twisted with respect to the tube axis.

We can now show explicitly that the helicity of a purely toroidal field $B^1\mathbf{e}_1$ is zero. for then

$$\sqrt{g}\, B^3 = \frac{\partial\tilde{\psi}}{\partial s} + \frac{1}{L}\frac{\partial P}{d\chi} = 0\,, \tag{3.16}$$

so that

$$\tilde{\psi} = -\frac{s}{L}\frac{dP}{d\chi} + f(\chi,\phi) \tag{3.17}$$

for some $f(\chi,\phi)$ periodic in ϕ. But $\tilde{\psi}$ is periodic in s, hence $dP/d\chi = 0$, i.e. $P \equiv 0$. Hence from (3.13), $\mathcal{H}(\chi) \equiv 0$. Similarly for a purely poloidal field $T \equiv 0$ and so again $\mathcal{H}(\chi) \equiv 0$. Again, we emphasize that these results hold only by virtue of the fact that the poloidal field is defined with respect to the zero-framed coordinate system.

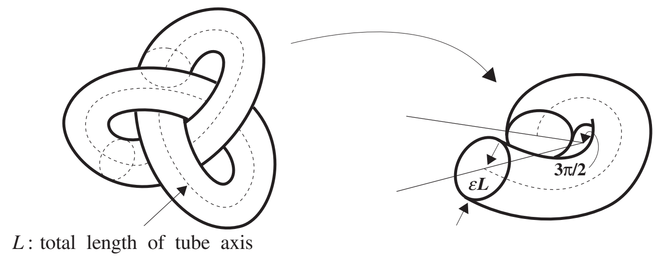

Figure 4. Trefoil knot in the 'pulled-tight' configuration for which the radius of curvature $\rho(s)$ of C is nowhere less than $2\epsilon L$.

4. Standard flux tube with prescribed helicity

It is useful in what follows to define a 'standard' flux tube knotted in the form of an arbitrary knot $\mathcal{K}$, carrying toroidal (or 'axial') flux Φ, and having prescribed total helicity $h\Phi^2$. A technique for achieving this using Dehn surgery (cutting, twisting and reconnecting) was described by Moffatt (1990a). Here, we obtain the form of the resulting field $\mathbf{B}$ referred to the system of coordinates (s, χ, ϕ) introduced above.

We first suppose that the shape function $R(s, \chi, \phi)$ is independent of both s and ϕ, so that (2.8) becomes simply

$$r = R(\chi)\,. \tag{4.1}$$

The tube is then uniform in structure along its length, and all magnetic surfaces have circular cross-sections ($s =$ cst., $\chi =$ cst.). The volume of the tube inside S_χ is

$$V(\chi) = \int_0^L ds \int_0^{2\pi} d\phi \int_0^\chi \sqrt{g}\, d\chi = \pi R^2(\chi) L\,. \tag{4.2}$$

We choose $V = \chi V_{\mathcal{T}}$ (see (2.1)), so that

$$R(\chi) = (V_{\mathcal{T}}\chi/\pi L)^{\frac{1}{2}} = \epsilon L \chi^{\frac{1}{2}} \tag{4.3}$$

where $\epsilon = (V_{\mathcal{T}}/\pi L^3)^{\frac{1}{2}}$. In practice, for any knotted flux tube, the parameter ϵ is small. Consider, for example, the trefoil knot in the 'pulled-tight' configuration shown in Figure 4. The cross-section is assumed circular with radius ϵL. The constraint of non-self-intersection implies that the radius of curvature $\rho(s)$ of the magnetic axis must be nowhere less than $2\epsilon L$. The tube can be cut into three equal portions each of length $L/3 \approx \overline{\rho}\Delta\theta$ where $\Delta\theta \gtrsim 3\pi/2$ and $\overline{\rho} > 2\epsilon L$. Hence, for this case,

$$\epsilon < (9\pi)^{-1} = 0{\cdot}035\,. \tag{4.4}$$

For any more complex knot, ϵ will be even smaller.

The standard flux tube is now defined by the choices of $T(\chi)$, $P(\chi)$:

$$\begin{cases} T(\chi) &= \Phi\chi\,, \\ P(\chi) &= h\Phi\chi\,. \end{cases} \tag{4.5}$$

To construct a particular field $\mathbf{B}_0$ with this signature, we substitute (4.1), (4.3) and (4.5) in (2.22), taking $\tilde{\psi} \equiv 0$. This gives

$$\mathbf{B}_0 = \frac{\Phi/V_{\mathcal{T}}}{1 - R(\chi)c(s)\cos(\phi - 2\pi\mathcal{N}s/L)}\,(L, 0, 2\pi h)\,. \tag{4.6}$$

Here the components B_0^1 and B_0^3 have different dimensions, but $B_0^1\mathbf{e}_1$ and $B_0^3\mathbf{e}_3$ have the same dimensions (those of flux divided by area) as required. The total helicity of the field $\mathbf{B}_0$ is, from (3.15), given by

$$\mathcal{H} = h\Phi^2. \tag{4.7}$$

The parameter h may be interpreted as $(2\pi)^{-1}$ times the angle of twist required to generate the poloidal field (4.5b) from the toroidal field (4.5a), starting from a situation with $P = 0$. We may therefore refer to h as the 'twist parameter' of the standard flux tube.

5. Minimisation of magnetic energy

Consider now the magnetic energy of the field

$$\mathcal{M} = \tfrac{1}{2}\int_{\mathcal{T}} \mathbf{B}^2\,dV\,. \tag{5.1}$$

We suppose that the flux tube $\mathcal{T}$ is immersed in a perfectly conducting incompressible fluid; its signature

$$S = \{V(\chi)\,,\,T(\chi)\,,\,P(\chi)\} \tag{5.2}$$

is then invariant under volume-preserving frozen-field distortions (Moffatt 1990b). Moreover the knot type $\mathcal{K}$ of the magnetic axis is invariant, and the tube $\mathcal{T}$ must not intersect itself. We seek to minimise $\mathcal{M}$ subject to these constraints, the minimum then corresponding to a state of stable magnetostatic equilibrium. Note that the volume $V(\chi)$ is given by

$$V(\chi) = \int_0^{2\pi}\int_0^{\chi}\int_0^{L}\sqrt{g}\,ds\,d\chi\,d\phi\,, \tag{5.3}$$

or equivalently, using (2.14),

$$\frac{dV}{d\chi} = \int_0^{2\pi}\int_0^{L} RR_\chi(1 - R\,c(s))\cos(\phi - 2\pi\mathcal{N}s/L)\,ds\,d\phi\,. \tag{5.4}$$

Also, defining

$$b_1 = \sqrt{g}\,B^1 = -\tilde{\psi}_\phi + T'/2\pi\,, \quad b_3 = \sqrt{g}\,B^3 = \tilde{\psi}_s + P'/L\,, \tag{5.5}$$

we have

$$\mathcal{M} = \frac{1}{2}\iiint \frac{1}{\sqrt{g}}\left(b_1^2\,g_{11} + 2b_1b_3\,g_{13} + b_3^2\,g_{33}\right)ds\,d\chi\,d\phi\,. \tag{5.6}$$

$\mathcal{M}$ is a function of $\tilde{\psi}$ (through b_1 and b_3), of R (through the constraint (5.4)) and of $\mathbf{X}(s)$ (through g_{ij}); the problem is thus to determine $\tilde{\psi}$, R and $\mathbf{X}(s)$ such that $\mathcal{M}$ is minimised subject to the above constraints.

This variational problem is extremely difficult, and in order to make progress it is necessary to impose additional mild constraints on the class of field structures to be considered. The minimum energy thus obtained will be greater than the true minimum, but will at least provide an upper bound on this. The field structures determined by this procedure are 'constrained magnetostatic equilibria'; if the constraints are removed, then in general the field will evolve to a lower energy state of true magnetostatic equilibrium. This evolution may involve simply a small adjustment, or it may involve an instability with relatively large associated reduction of magnetic energy. We shall comment further on these possibilities below.

(*a*) *Axially uniform flux tubes*

The first additional constraint that we impose is that the flux tube be uniform along its length, i.e. that $\tilde{\psi}$ and R be independent of s. The magnetic surfaces $\chi = \chi(r, \phi)$ are then the same at every section s, and $\mathbf{B}$ depends on s only through the dependence of g_{ij} on $c(s)$ and $\tau(s)$. Under this assumption, (5.5) gives

$$b_1 = \Lambda(\chi, \phi) + T'(\chi)/2\pi\,, \quad b_3 = P'(\chi)/L\,, \tag{5.7}$$

where $\Lambda(\chi, \phi) = -\tilde{\psi}_\phi$; since $\tilde{\psi}$ is periodic in ϕ,

$$\int_0^{2\pi} \Lambda(\chi, \phi)\, d\phi = 0\,. \tag{5.8}$$

Since b_1 and b_3 are now independent of s, (5.6) now gives

$$\mathcal{M} = \tfrac{1}{2} \iint \left(\kappa_{11} b_1^2 + 2\kappa_{13}\, b_1\, b_3 + \kappa_{33}\, b_3^2\right)\, d\chi d\phi\,, \tag{5.9}$$

where

$$\kappa_{ij}(\chi, \phi) = \oint \frac{g_{ij}}{\sqrt{g}}\, ds\,. \tag{5.10}$$

Substituting (5.7) in (5.9), we now obtain $\mathcal{M}$ in the form

$$\mathcal{M} = \frac{1}{2} \iint \left(A\Lambda^2 + 2B\Lambda + C\right) d\chi\, d\phi\,, \tag{5.11}$$

where

$$\left\{ \begin{array}{lcl} A &=& \kappa_{11}\,, \\ B &=& \kappa_{11} T'/2\pi + \kappa_{13}\, P'/L\,, \\ C &=& \kappa_{11}(T'/2\pi)^2 + \kappa_{13} T' P'/\pi L + \kappa_{33}(P'/L)^2\,. \end{array} \right. \tag{5.12}$$

We may now partially minimise $\mathcal{M}$ with respect to Λ, subject to the constraint (5.8). This is achieved in straightforward manner by introducing a Lagrange multiplier $\lambda(\chi)$ and minimising

$$\tfrac{1}{2}(A\Lambda^2 + 2B\Lambda + C) - \lambda(\chi)\Lambda(\chi, \phi)\,. \tag{5.13}$$

This gives

$$\Lambda = \frac{\lambda - B}{A}\,, \quad \lambda = \int \frac{B\, d\phi}{A} \Big/ \int \frac{d\phi}{A}\,. \tag{5.14}$$

Hence the partially minimised energy is obtained in the form

$$\mathcal{M}^*\{\mathbf{X}, R\} = \frac{1}{2} \int_0^1 \left(G(\chi) + H(\chi)\right) d\chi\,, \tag{5.15}$$

where

$$G(\chi) = \left(T' + \frac{P'}{L}\int_0^{2\pi} \frac{\kappa_{13}}{\kappa_{11}}\,d\phi\right)^2 \Big/ \int_0^{2\pi} \frac{d\phi}{\kappa_{11}}\,, \tag{5.16}$$

and

$$H(\chi) = \left(\frac{P'}{L}\right)^2 \int_0^{2\pi} \left(\kappa_{33} - \frac{\kappa_{13}^2}{\kappa_{11}}\right) d\phi\,. \tag{5.17}$$

The 'uniform flux tube' constraint seems reasonable for any flux tube whose cross-sectional radius δ is everywhere small compared with $1/c(s)$; however, if the constraint is removed, the tube may be subject to 'ballooning' instabilities or to kink-mode instabilities which increase $c(s)$; in either case, evolution to a significantly lower energy state may occur.

(*b*) *Flux tubes with circular cross-section*

The second additional constraint that we may impose is that the shape function R be independent of ϕ; then (cf. (4.1)–(4.3)), with the choice $V(\chi) = \chi V_{\mathcal{T}}$, the constraint (5.4) gives

$$R(\chi) = \epsilon L \chi^{\frac{1}{2}}\,, \tag{5.18}$$

where $\epsilon = (V_{\mathcal{T}}/\pi L^3)^{\frac{1}{2}}$, and we have seen in §4 that, for any knotted tube, ϵ is necessarily quite small. The metric tensor (2.13) then simplifies to

$$(g_{ij}) = \begin{pmatrix} (1-\epsilon L\chi^{\frac{1}{2}} c\cos\theta)^2 + \epsilon^2 L^2 \chi \tau^{*2} & 0 & \epsilon^3 L^2 \chi \tau^* \\ 0 & \epsilon^2/4\chi & 0 \\ \epsilon^2 L^2 \chi \tau^* & 0 & \epsilon^2 L^2 \chi \end{pmatrix} \tag{5.19}$$

and

$$\sqrt{g} = \frac{1}{2}\epsilon^2 L^2 (1 - \epsilon L \chi^{\frac{1}{2}}\, c\cos\theta)\,. \tag{5.20}$$

The 'circular cross-section' constraint also appears to be reasonable provided $\delta c(s) \ll 1$. If this constraint alone is removed, then a small adjustment of cross-section away from circular symmetry is to be expected (in response to the effects of local curvature and torsion) but such adjustment will involve only a small decrease of magnetic energy.

There are two circumstances in which further substantial progress may be made: (a) if c and τ are constants, then the κ_{ij} may be evaluated, and are independent of ϕ; hence the functions $G(\chi)$ and $H(\chi)$ in (5.15) and (5.16) may be greatly simplified. This is the case of a helical flux tube with periodic end conditions; we treat this case in detail in §6. (b) If, for a knotted tube, we exploit the fact that ϵ is small, we may expand $\mathcal{M}^*\{\mathbf{X}, R\}$ as a power series in ϵ^2 and then seek minimum energy states within a prescribed class of curves $\mathbf{X}(s)$ of given knot type. We follow this procedure in §§7 and 8 in determining the minimum energy function $\overline{m}(h)\Phi^2 V^{-\frac{1}{3}}$ for torus knots.

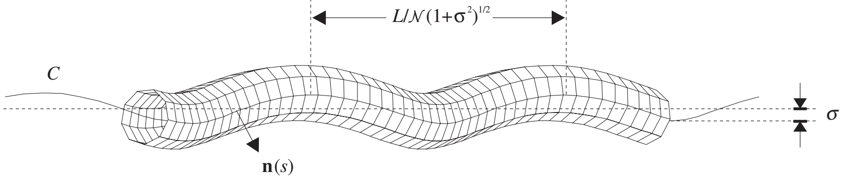

Figure 5. Helical flux tube with constant curvature and torsion; periodic end conditions are imposed. For the 'free' situation, L is constant; for the 'line-tied' situation, $z_0 = L(1+\sigma^2)^{-\frac{1}{2}}$ is constant.

6. Helical flux tubes and kink-mode instabilities

Consider a helical flux tube (Figure 5) whose magnetic axis C is the helix

$$\mathbf{X}(s) = \frac{1}{\sqrt{1+\sigma^2}}\left(\frac{\sigma}{k}\cos ks\,,\ \frac{\sigma}{k}\sin ks\,,\ s\right), \tag{6.1}$$

where

$$k = 2\pi\mathcal{N}/L\,. \tag{6.2}$$

For definiteness, we suppose that $k > 0$, $\sigma > 0$, so that the helix is right-handed. This curve is not closed, but it satisfies the periodicity condition $\mathbf{X}(s+L) = \mathbf{X}(s)$, and this is sufficient for present purposes. The unit principal normal is

$$\mathbf{n}(s) = (-\cos ks\,,\ -\sin ks\,,\ 0)\,, \tag{6.3}$$

and this makes $\mathcal{N}$ complete rotations as s increases from zero to L. The curvature and torsion of C are easily found to be

$$c = \frac{k\sigma}{\sqrt{1+\sigma^2}}\,, \quad \tau = \frac{k}{\sqrt{1+\sigma^2}}\,, \tag{6.4}$$

and both are constant.

We consider a flux-tube that is uniform in s and of circular cross-section, so that as in §5,

$$R(\chi) = \epsilon L\chi^{\frac{1}{2}}\,, \quad \epsilon = (V_{\mathcal{T}}/\pi L^3)^{\frac{1}{2}}\,. \tag{6.5}$$

The only restriction that we place on ϵ is (2.16), i.e.

$$p = \epsilon Lc < 1\,. \tag{6.6}$$

We wish to evaluate κ_{ij} exactly; thus

$$\kappa_{11} = \frac{2}{\epsilon^2 L} + 2\chi\tau^{*^2}\int_0^L \frac{ds}{1-\epsilon Lc\chi^{\frac{1}{2}}\cos(\phi - ks)} = \frac{2}{\epsilon^2 L} + \frac{2L\tau^{*^2}\chi}{\sqrt{1-\epsilon^2L^2c^2\chi}}\,. \tag{6.7}$$

Similarly,

$$\kappa_{13} = \tau^*\kappa_{33} = \frac{2L\tau^*\chi}{\sqrt{1-\epsilon^2L^2c^2\chi}}\,. \tag{6.8}$$

Since the κ_{ij} are independent of ϕ, we now obtain from (5.14)–(5.16)

$$\mathcal{M}^* = \pi\int_0^1\left[\kappa_{11}\left(\frac{T'}{2\pi}\right)^2 + 2\kappa_{13}\left(\frac{T'}{2\pi}\right)\left(\frac{P'}{L}\right) + \kappa_{33}\left(\frac{P'}{L}\right)^2\right]d\chi \tag{6.9}$$

which can be further reduced to

$$\mathcal{M}^* = \frac{1}{2\pi\epsilon^2 L}\int_0^1 T'^2\, d\chi + 2\pi L\int_0^1 \left(\tau^* \frac{T'}{2\pi} + \frac{P'}{L}\right)^2 \frac{\chi d\chi}{\sqrt{1-p^2\chi}} \tag{6.10}$$

using (6.7) and (6.8), where p is defined by (6.6).

The structure of this expression now indicates the manner in which a straight tube (for which $\sigma = 0$) may be unstable to helical deformation. As σ increases from zero, the quantity

$$\tau^* = \tau - k = k[(1+\sigma^2)^{-\frac{1}{2}} - 1] \tag{6.11}$$

varies between zero and $-k$, and the consequent variation of the factor

$$\left(\tau^* \frac{T'}{2\pi} + \frac{P'}{L}\right)^2$$

in (6.10) may be such as to decrease $\mathcal{M}^*$.

This may be seen explicitly for the case of the standard flux tube (where $P' = hT' = h\Phi$) for which (6.10) reduces further to

$$\mathcal{M}^* = \frac{\Phi^2}{2\pi\epsilon^2 L}\left\{1 + \epsilon^2 L^2 (\tau^* + 2\pi h L)^2 F(p)\right\} \tag{6.12}$$

where

$$F(p) = \int_0^1 \frac{\chi d\chi}{\sqrt{1-p^2\chi}} = \frac{2}{3p^4}\left(2 - (2+p^2)\sqrt{1-p^2}\right). \tag{6.13}$$

We now consider two different cases: (a) instability of a flux tube with constant length and (b) instability of a line-tied flux tube.

(*a*) *Flux tube with constant length*

In this case L is a constant; the function $F(p)$ is monotonic increasing in the range $0 < p < 1$ between its limiting values

$$F(0) = 1/2\,, \quad F(1) = 4/3\,. \tag{6.14}$$

Hence, if $\tau - k + 2\pi h/L$ vanishes for any value of τ in the accessible range $(0, k)$, then $\mathcal{M}^*$ is minimal for that value (and for the corresponding value of σ). This condition is satisfied if

$$0 < h < Lk/2\pi = \mathcal{N}\,; \tag{6.15}$$

and the corresponding helical configuration is then characterised by the values

$$\tau = \frac{2\pi}{L}(\mathcal{N} - h)\,, \quad c = \frac{2\pi}{L}(h^2 - 2\mathcal{N}h)^{\frac{1}{2}}\,, \quad \sigma = \frac{(h^2 - 2\mathcal{N}h)^{\frac{1}{2}}}{\mathcal{N} - h}\,. \tag{6.16}$$

The cylindrical state with $\sigma = 0$ is an equilibrium, but this is unstable if

$$(\partial\mathcal{M}^*/\partial\sigma^2)_{\sigma=0} < 0\,. \tag{6.17}$$

From (6.11), (6.12) and (6.13), this criterion yields as a condition for instability

$$0 < h\mathcal{N}\epsilon^2 < \frac{3}{4\pi^2}\,. \tag{6.18}$$

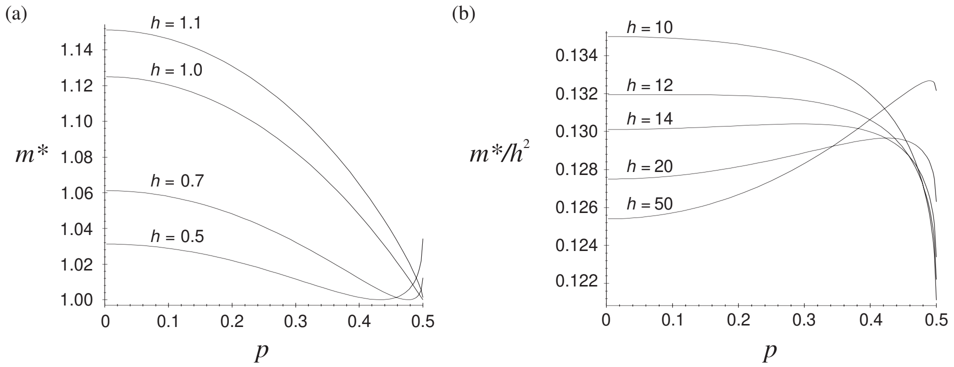

Figure 6. The energy function $m^*(p)$ for the free state with $\mathcal{N} = 1$, $\epsilon = (4\pi)^{-1}$, for various values of h. (a) Note the loss of stability at $p = 0$ (i.e. $\sigma = 0$) as h increases through unity. (b) Note the appearance of a new constrained equilibrium state when h increases through the critical value $h_c = 12$ (from (6.18)).

This type of instability has been found previously (Anzer 1968). However the alternative lower energy states (6.16) (for $\mathcal{N} = 1, 2, 3, ...$) are believed to be new.

By way of illustration, consider the particular case $\mathcal{N} = 1$, $\epsilon = (4\pi)^{-1}$. The critical value of h as given by (6.18) is $h_c = 12$. The corresponding range of p is $0 \leqslant p \leqslant \frac{1}{2}$, and (6.12) gives

$$m^* = \frac{LM^*}{8\pi\Phi^2} = 1 + \frac{1}{4}\left(\sqrt{1 - 4p^2} + h - 1\right) F(p) \,. \tag{6.19}$$

Figure 6 shows m^* as a function of p for various values of h, indicating the manner in which the minimum energy state changes as h increases. Note however that this is just for $\mathcal{N} = 1$. Other modes with $\mathcal{N} \geqslant 2$ may be unstable for values of h for which the $\mathcal{N} = 1$ mode is stable.

The expression (6.10) may be used to analyse the stability of flux tubes of arbitrary signature $\{T(\chi), P(\chi)\}$. This topic is important in the context of plasma containment, and will be treated in a separate paper.

(*b*) *Line-tied equilibria*

The situation is rather different if the field lines are 'tied' at fixed planes $z = 0$ and $z = z_0$ (as considered by Hood & Priest 1979). In this case,

$$L = z_0\sqrt{1 + \sigma^2}\,, \tag{6.20}$$

and we must take account of this variation of L with σ in considering the energy functional $\mathcal{M}^*$. We may take as unit of length $z_0 = 1$, so that $L \geqslant 1$. With $\epsilon = (V/\pi)^{\frac{1}{2}}\, L^{-\frac{3}{2}}$, (6.12) gives

$$m^* = \frac{2V}{\Phi^2}\mathcal{M}^* = L^2 + \frac{4\pi\mathcal{N}^2 V}{L}\left(\sqrt{1 - \frac{p^2L^3}{4\pi\mathcal{N}^2 V}} + \frac{h}{\mathcal{N}} - 1\right)^2 F(p)\,, \tag{6.21}$$

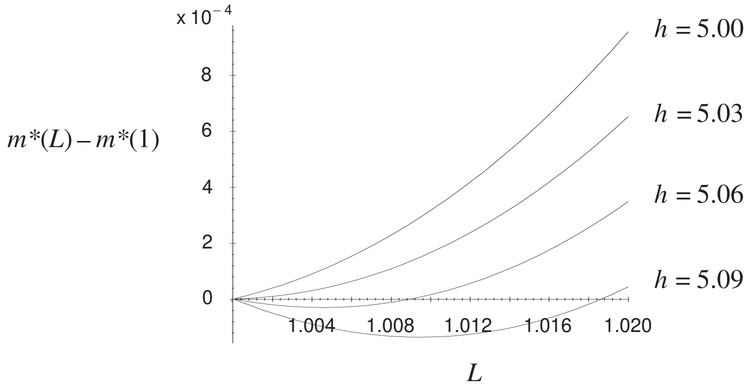

Figure 7. The energy function $m^*(L) - m^*(1)$ for the line-tied state with $\mathcal{N} = 3$, $V = \pi/400$. Note the change of stability of the state $L = 1$ (i.e. $\sigma = 0$) when h increases through the critical value $h_c = 5.03$.

and p is related to L through

$$\begin{aligned} p &= \epsilon L c = 2(\pi V)^{\frac{1}{2}} \mathcal{N} \sigma (1+\sigma^2)^{-\frac{5}{4}} \\ &= 2(\pi V)^{\frac{1}{2}} \mathcal{N} (L^2-1)^{\frac{1}{2}} L^{-\frac{5}{2}} . \end{aligned} \tag{6.22}$$

The quantity $m^*(L) - m^*(1)$ is plotted in Figure 7 as a function of L for $\mathcal{N} = 3$, $V = \pi/400$. This indicates a change of stability of the cylindrical state ($L = 1$) when h increases through the critical value $h_c \approx 5.03$. For $h > h_c$, a new constrained helical equilibrium is established as indicated by the corresponding minimum of $m^*(L)$.

There are essentially three constraints in the above treatment of helical flux tubes: (i) the uniform flux constraint; (ii) the circular cross-section constraint; and (iii) the constraint that the magnetic axis should be one of the two-parameter family of helices (6.1). If constraint (i) alone is removed, the equilibrium should survive because a uniform flux tube is compatible with uniform curvature and torsion. If constraint (ii) alone is removed, then a small but uniform adjustment of cross-section is to be expected; and if the constraint (iii) alone is removed, then 'superkink' type instabilities may conceivably deform C out of the two-parameter family (6.1), with a possibly large reduction of magnetic energy.

7. Expansion of $\mathcal{M}^*$ in powers of ϵ^2

As observed in §4, the parameter $\epsilon = (V_{\mathcal{T}}/\pi L^3)^{\frac{1}{2}}$ is necessarily small for a knotted flux tube. It makes sense therefore to expand the expression (5.14) for $\mathcal{M}^*$ as a power series in ϵ. We find that

$$\mathcal{M}^* = \frac{1}{\epsilon^2}\left(m_0 + m_2\epsilon^2 + \cdots\right) \tag{7.1}$$

where the coefficients m_0 and m_2 are determined below (Eqns. (7.12) and (7.13)); here and subsequently, $+\cdots$ indicates terms that may be neglected.

First, we need to calculate $\kappa_{11}(\chi,\phi)$. From (5.17) and (5.18), we have

$$\frac{g_{11}}{\sqrt{g}} = \frac{2}{\epsilon^2 L^2}\left(1 - \epsilon L \chi^{\frac{1}{2}} c(s)\cos\theta + \epsilon^2 L^2 \chi \tau^{*^2} + \cdots\right). \tag{7.2}$$

Here,

$$\cos\theta = \cos(\phi + 2\pi\mathcal{N}s/L) = \cos\phi\cos(2\pi\mathcal{N}s/L) - \sin\phi\sin(2\pi\mathcal{N}s/L), \tag{7.3}$$

so that

$$\begin{aligned}\kappa_{11}(\chi,\phi) &= \oint \frac{g_{11}}{\sqrt{g}}\, ds \\ &= \frac{2}{\epsilon^2 L}\left(1 - \tfrac{1}{2}\epsilon\chi^{\frac{1}{2}} L(a_{\mathcal{N}}\cos\phi - b_{\mathcal{N}}\sin\phi) + \epsilon^2 L^2 \chi \oint \tau^{*2} ds + \cdots\right),\end{aligned} \tag{7.4}$$

where $a_{\mathcal{N}}$ and $b_{\mathcal{N}}$ are the $\mathcal{N}$th Fourier coefficients of $c(s)$, i.e.

$$a_{\mathcal{N}} = \frac{2}{L}\int_0^L c(s)\cos(2\pi\mathcal{N}s/L)\, ds, \quad b_{\mathcal{N}} = \frac{2}{L}\int_0^L c(s)\sin(2\pi\mathcal{N}s/L)\, ds. \tag{7.5}$$

Hence,

$$\oint \frac{d\phi}{\kappa_{11}} = \pi\epsilon^2 L\left(1 + \tfrac{1}{8}\epsilon^2\chi L^2 |c_{\mathcal{N}}|^2 - \epsilon^2 L\chi \oint \tau^{*2}\, ds + \cdots\right), \tag{7.6}$$

where

$$c_{\mathcal{N}} = a_{\mathcal{N}} + i b_{\mathcal{N}} = \frac{2}{L}\int_0^L c(s)\exp(2\pi i\mathcal{N}s/L)\, ds. \tag{7.7}$$

Secondly, we need to calculate κ_{13} and κ_{33}; however, since these are both $O(1)$, we need only calculate the leading terms of the integrals

$$\int_0^{2\pi} \frac{\kappa_{13}}{\kappa_{11}}\, d\phi = 2\pi\epsilon^2 L\chi \oint \tau^* ds + \cdots, \tag{7.8}$$

$$\int_0^{2\pi}\left(\kappa_{33} - \frac{\kappa_{13}^2}{\kappa_{11}}\right) d\phi = 2\pi\chi L + \cdots. \tag{7.9}$$

For simplicity, we now restrict attention to the standard flux tube for which $P' = hT' = h\Phi$. Substitution of (7.6), (7.8) and (7.9) in (5.15) and (5.16) then gives

$$G(\chi) = \frac{\Phi^2}{\pi\epsilon^2 L}\left[1 + \epsilon^2\chi\left(4\pi h \oint \tau^*\, ds + \oint \tau^{*2} ds - \frac{1}{8}L^2|c_{\mathcal{N}}|^2\right)\right] + \cdots, \tag{7.10}$$

$$H(\chi) = 4\pi h^2 \Phi^2 \chi/L + \cdots. \tag{7.11}$$

Hence finally from (5.14), we obtain the result (7.1) with

$$m_0 = \Phi^2/2\pi L, \tag{7.12}$$

$$m_2 = \frac{\Phi^2}{4\pi L}\left(\oint\left(\tau^* + \frac{2\pi h}{L}\right)^2 ds - \frac{1}{8}L^2|c_{\mathcal{N}}|^2\right). \tag{7.13}$$

Once again, we note the appearance of the factor $(\tau^* + 2\pi h/L)^2$ (cf. Eqn. (6.11) for the case of the helix). Thus, again, $\mathcal{M}^*$ is decreased by deformations that

$T_{4,3}$

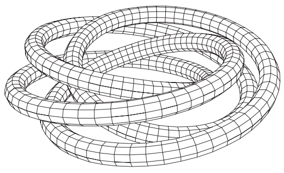

Figure 8. Flux tube in the form of the torus knot $T_{4,3}$.

reduce the mean-square value of $\tau^* + 2\pi h/L$ on C. Now, however, we note an additional new, and somewhat surprising, phenomenon: an increase of curvature on the scale $L/2\pi\mathcal{N}$ increases $|c_{\mathcal{N}}|$ and therefore tends to *decrease* m_2. Under general deformations of C, however, there may be a trade-off between the positive and negative contributions to (7.13), and it is the balance between these effects that determines the minimising configuration.

We have supposed throughout that C has no points of inflexion. We may now, however, consider what happens if C is continuously deformed in such a way that an inflexion point $s = s^*$ appears at one instant $t = t^*$, say. As shown by Moffatt & Ricca (1992), both $\mathcal{N}$ and $(2\pi)^{-1} \oint \tau ds$ are discontinuous in the passage through this inflexion, but in just such a way that the quantity

$$\mathcal{T}^* = \frac{1}{2\pi} \oint \tau^* \, ds = \frac{1}{2\pi} \oint \tau ds - \mathcal{N} \tag{7.14}$$

varies continuously. However, the integral $\oint \tau^{*^2} \, ds$ diverges as C approaches the inflexional configuration, so that $\kappa_{11}(\chi, \phi)$ is then undefined. The coordinate system (s, χ, ϕ) is simply not appropriate to deal with this situation.

8. Torus knot flux tubes

Let us now apply the above results to the situation in which the magnetic axis C is a torus knot $T_{m,n}$ with parametric representation

$$\mathbf{X}(t) = R((1 + \lambda \cos nt) \cos mt,\ (1 + \lambda \cos nt) \sin mt,\ \lambda \sin nt) \tag{8.1}$$

for $0 \leqslant t \leqslant 2\pi$ (Figure 8). We suppose $\lambda > 0$ so that the knot is *left-handed.* Note that the arc length s is related to the parameter t by

$$ds = R\sqrt{\lambda^2 n^2 + m^2(1 + \lambda \cos nt)^2} \, dt \,, \tag{8.2}$$

and the length of C is given by

$$L = R \int_0^{2\pi} \sqrt{\lambda^2 n^2 + m^2(1 + \lambda \cos nt)^2} \, dt = R\ell(\lambda) \ , \ \text{say.} \tag{8.3}$$

We need first to compute the 'separation function'

$$d(u, v) = |\mathbf{X}(u) - \mathbf{X}(v)| \tag{8.4}$$

(shown in Figure 9b for the case of the trefoil knot $T_{2,3}$). This function has local minima for values of (u, v) where the curve approaches 'near to itself'. Let $d_{\min}$ be the least of these minima (other than zero) (Figure 9a). Clearly, $d_{\min}$ has the

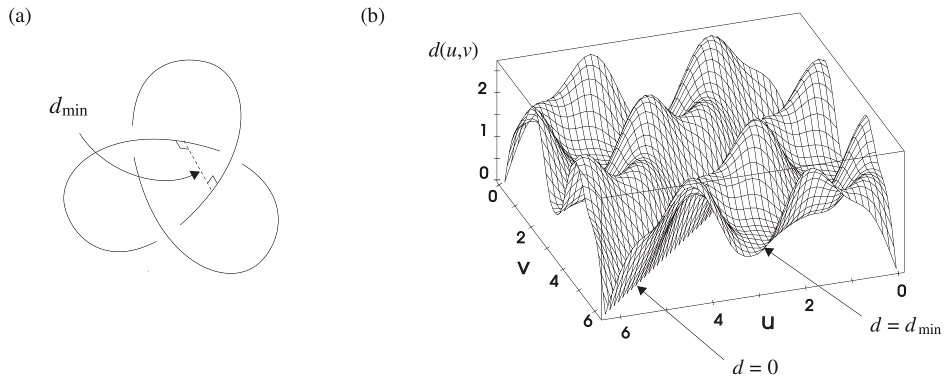

Figure 9. (a) Local minimum $d_{\min}$ of the separation function $d(u,v)$ for the trefoil knot $T_{2,3}$. (b) Surface plot of $d(u,v) = \text{cst.}$ for $T_{2,3}$ ($R = 1$, $\lambda = 0.4$).

form

$$d_{\min} = R\tilde{d}(\lambda) \tag{8.5}$$

for some function $\tilde{d}(\lambda)$; for small λ, this function has the form $\tilde{d}(\lambda) \approx 2\lambda \sin(\pi/m)$.

We may now construct a standard flux tube around C of radius ϵL, and provided

$$\epsilon L \leqslant d_{\min}\,, \tag{8.6}$$

it is clear that this flux tube is non-self-intersecting. In the 'pull-tight' situation in which the toroidal energy is minimised, the tube makes contact with itself, i.e. $\epsilon L = d_{\min}$; this 'contact condition' may be written in the equivalent form

$$R^3 = \frac{4V_{\mathcal{T}}}{\pi \ell(\lambda)(d(\lambda))^2} \tag{8.7}$$

and thus, for given $V_{\mathcal{T}}$, determines R in terms of λ.

The energy function $\mathcal{M}^*$ given by (7.1), (7.12) and (7.13) may now be readily computed as a function of R and λ, and hence using (8.7) as a function of λ alone; we may then minimise with respect to λ obtaining $\mathcal{M}_{\min}$ in the form

$$\mathcal{M}_{\min} = \overline{m}(h)\Phi^2 V_{\mathcal{T}}^{-\frac{1}{3}}. \tag{8.8}$$

The function $\overline{m}(h)$ is shown in Figure 10 for the two representations $T_{2,3}$ and $T_{3,2}$ of the trefoil knot. As anticipated, these curves exhibit minima for non-zero values of h, ($h \approx 6$, $\overline{m}_{\min} \approx 32$ for $T_{2,3}$; $h \approx 0{\cdot}11$, $\overline{m}_{\min} \approx 36{\cdot}3$ for $T_{3,2}$) consistent with the conjecture of Moffatt (1990a). Note however the unexpected result that for $h \lesssim 2{\cdot}3$, the $T_{3,2}$ representation has lower energy than the $T_{2,3}$ representation.

Figure 11 shows the function $\overline{m}(h)$ for torus knots $T_{2,n}$ ($n = 3, 5, 7, 9$). For moderate values of $h (\lesssim 10)$ the energy increases with n, i.e. with knot complexity. For larger values of h the results are unreliable, because the contact condition (8.7) need not be satisfied; moreover, just as for the case of the helical flux tube, the torus-knot tube may be subject to local kink-mode instabilities so that the simple representation (8.1) of the magnetic axis is no longer valid. These more complex effects will be considered in a separate paper.

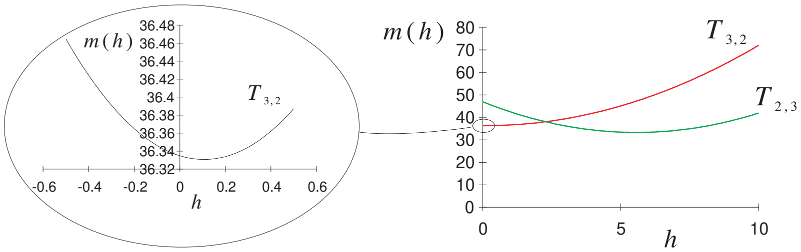

Figure 10. The minimum energy function $\overline{m}(h)$ for two representations of the trefoil knot, $T_{2,3}$ and $T_{3,2}$.

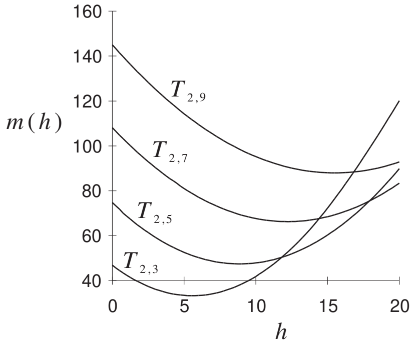

Figure 11. The minimum energy function $\overline{m}(h)$ for torus knots $T_{2,n}$ $(n = 3, 5, 7, 9)$; for $h \lesssim 10$, the knot energy increases with increasing knot complexity.

9. Summary and conclusions

In this paper, we have developed a general technique whereby constrained minimum energy states of knotted magnetic flux tubes may be identified. This technique first involves definition of an appropriate (non-orthogonal) curvilinear coordinate system in the neighbourhood of a closed curve C, under the condition that C has no points of vanishing curvature. This coordinate system is 'zero-framed' with respect to C, with the consequence that a natural toroidal-poloidal decomposition of the field $\mathbf{B}$ in a flux tube $\mathcal{T}$ around C can be established. The field is assumed to have magnetic surfaces $\chi =$ cst. nested around C (the magnetic axis) and is characterised by a signature $\{V(\chi), T(\chi), P(\chi)\}$ where V is volume, T is toroidal flux and P poloidal flux inside the surface labelled χ. The decomposition is natural in that the helicity of either a purely toroidal or a purely poloidal field is zero; the helicity function $\mathcal{H}(\chi)$ is given by Eqn.(3.12), the appropriate generalisation to knotted flux tubes of a result first discerned by Kruskal & Kulsrud (1958).

In §5, we have used the above coordinate system in order to obtain an expression for the magnetic energy $\mathcal{M}$ of the field $\mathbf{B}$ in terms of its signature and the parametric representation of C. Following the variational principle of Bernstein *et al* (1958), but here applied to volume-preserving deformations, we have then sought to minimise $\mathcal{M}$ while conserving both the signature of the field and the topology of C. To make progress, we introduced two mild constraints, restricting attention to axially uniform tubes of circular cross-section; and we obtained explicit results for the case of the *standard flux tube*, for which $V(\chi) = \chi V_{\mathcal{T}}$, $P(\chi) = hT(\chi) = h\Phi\chi$; here h is the twist parameter, and the total helicity of the field is $h\Phi^2$.

We first considered (in §6) the case of a helical flux tube with periodic end conditions. The fact that both curvature c and torsion τ are constant in this case allows explicit evaluation of the (constrained) minimum magnetic energy as a function of these parameters, or equivalently of the parameters (k, σ) related to (c, τ) by (6.4). New lower energy helical equilibrium states have been identified in circumstances where the cylindrical magnetostatic equilibrium ($\sigma = 0$) is unstable. Criteria for instability have been obtained for both 'free' and 'line-tied' cylindrical equilibria, in broad agreement with earlier investigations of Anzer (1968) and Hood & Priest (1979). These results inspire confidence in the validity and viability of the technique.

In §8, the technique is applied to situations in which the flux tube has the form of a torus knot $T_{m,n}$, the curve C having parametric representation (8.1). The magnetic energy of the standard flux tube depends on the parameters R and λ, and these are assumed related by the contact condition (8.7). The energy is then minimised with respect to the single independent parameter λ, and the dimensionless energy function $\overline{m}(h)$ in the relation $\mathcal{M}_{\min} = \overline{m}(h)\Phi^2 V_{\mathcal{T}}^{-1/3}$ is thus determined for a variety of torus knots of low order. These results, displayed in Figures 10 and 11, are broadly as anticipated by Moffatt (1990a), although the fact that, for small h, the value of $\overline{m}(h)$ is smaller for $T_{3,2}$ than for $T_{2,3}$ (the trefoil knot in two different geometrical configurations) is unexpected. The function $\overline{m}(h)$ provides an upper bound on the function $m(h)$ that applies when the constraints on tube structure and on the configuration (8.1) of the axis are removed. Recall that a lower bound is provided by the work of Freedman & He (1991).

The technique, as developed in this paper, may be applied to any knotted flux tube of volume $V_{\mathcal{T}}$ whose axis C may be represented in parametric form

$$\mathbf{X} = \mathbf{X}(t; \lambda, \mu, \ldots)\,, \tag{9.1}$$

where t is the parameter on C (related to arc-length), and $\lambda, \mu, \ldots$ are further geometrical parameters on which the magnetic energy $\mathcal{M}^*$ will depend, and with respect to which $\mathcal{M}^*$ may be minimised, subject to a contact condition of the form

$$\mathcal{C}(\lambda, \mu, \ldots) = V_{\mathcal{T}}\,. \tag{9.2}$$

The sole limitation on the technique is that the curve (9.1) must have no inflexion point (i.e. no point of vanishing curvature), since otherwise the coordinate system used is ill-defined. A technique which can cope with deformation through inflexional configurations provides an interesting, albeit elusive, target for future investigation.

AYKC would like to thank the Croucher Foundation (UK) for a 3-year scholarship. The work has been partially supported under EPSRC Contract GR/J21439.

REFERENCES

Anzer, U. 1968 The stability of force-free magnetic fields with cylindrical symmetry in the context of solar flares, *Solar Phys.* **3**, pp. 298–315.

Arnol'd, V.I. 1974 The asymptotic Hopf invariant and its applications (in Russian). In *Proc. Summer School in Differential Equations, Erevan.* Armenian SSR Acad. Sci., Transl. 1986 in *Sel. Math. Sov.* **5**, pp. 327–345.

Bateman, G. 1978 *MHD instabilities*, M.I.T. Press.

Berger, M.A. & Field, G.B. 1984 The topological properties of magnetic helicity. *J. Fluid Mech.* **147**, pp. 133–148.

Bernstein, I.B., Frieman, E.A., Kruskal, M.D. & Kulsrud, R.M. 1958 An energy principle for hydromagnetic stability problems. *Proc. Roy. Soc. (London)*, **A244**, pp. 17–40.

Bradbury, T.C. 1984 Mathematical methods with applications to problems in the physical sciences. John Wiley & Sons.

Chui, A.Y.K. & Moffatt, H.K. 1992 Minimum energy magnetic fields with toroidal topology. In *Topological Aspects of the Dynamics of Fluids and Plasmas* (eds. H.K. Moffatt *et al*), pp. 195–218. Kluwer.

Freedman, M.H. 1988 A note on topology and magnetic energy in incompressible perfectly conducting fluids. *J. Fluid Mech.* **194**, pp. 549–551.

Freedman, M.H. & He, Z.X. 1991 Divergence-free field: Energy and asymptotic crossing numbers. *Annal of Math.* **134**, pp. 189–229.

Hood, A.W. & Priest, E.R. 1979 Kink instability of solar coronal loops as the cause of solar flares. *Solar Phys.* **64**, pp. 303–321.

Kruskal, M.D. & Kulsrud, R.M. 1958 Equilibrium of a magnetically confined plasma in a toroid. *Phys. Fluids* **1**, pp. 265–274.

Moffatt, H.K. 1985 Magnetostatic equilibria and analogous Euler flows of arbitrarily complex topology. Part 1. Fundamentals. *J. Fluid Mech.* **159**, pp. 359–378.

Moffatt, H.K. 1990a The energy spectrum of knots and links. *Nature* **347**, pp. 367–369.

Moffatt, H.K. 1990b Structure and stability of solutions of the Euler equations: a Lagrangian approach. *Phil. Trans. R. Soc. Lond.* A **333**, pp. 321–342.

Moffatt, H.K. & Ricca, R.L. 1992 Helicity and the Călugăreanu invariant. *Proc. R. Soc. Lond.* A **439**, pp. 411–429.

Scharlemann, M. 1992 Topology of knots. In *Topological Aspects of the Dynamics of Fluids and Plasmas* (eds. H.K. Moffatt *et al*), pp. 195–218. Kluwer.